J Control Autom Electr Syst (2016) 27:169–178
DOI 10.1007/s40313-016-0228-4

Vector Control of Induction Motor Using an Integral Sliding Mode Controller with Anti-windup

Carlos M. R. Oliveira[1] · **Manoel L. Aguiar**[1] · **José R. B. A. Monteiro**[1] · **William C. A. Pereira**[1] · **Geyverson T. Paula**[1] · **Thales E. P. Almeida**[1]

Received: 18 September 2015 / Revised: 16 November 2015 / Accepted: 8 January 2016 / Published online: 29 January 2016

Abstract This work presents a sliding mode controller, applied to the three-phase induction motor using indirect field-oriented control technique. A possible approach for chattering reduction with high degree of robustness is based on the switching saturation function, although it presents steady-state error. This paper, therefore, proposes an integral sliding mode controller with a new anti-windup, which has low overshoot and no steady-state error. In addition, an approach using a switching sigmoid function is presented. The motor performance is verified by means of numeric simulations and experimental tests with load disturbances. The proposed controller presents better results when compared to other conventional sliding mode controllers and a tuned PI controller.

Keywords Integral sliding mode controller · Anti-windup · Induction motor

✉ Carlos M. R. Oliveira
carlosmro@usp.br

Manoel L. Aguiar
aguiar@sc.usp.br

José R. B. A. Monteiro
jrm@sc.usp.br

William C. A. Pereira
william.andrade@usp.br

Geyverson T. Paula
geyverson.paula@usp.br

Thales E. P. Almeida
thales.eugenio.almeida@usp.br

[1] São Carlos School of Engineering, University of São Paulo (USP), São Carlos, São Paulo, Brazil

1 Introduction

The three-phase induction motor (IM) is widely used in industrial applications due to its simple mechanical construction, reduced maintenance requirements and costs relative to the DC motor alternatives. However, the IM control is complex due to its nonlinear characteristics, coupled variables for flux and electromagnetic torque (Vas 1990).

The indirect field-oriented control (IFOC) has been widely used as a technique of control for IM, assuring steady-state decoupling of torque and flux control commands, so that the IM can be controlled similarly to a separately excited DC motor. However, the control performance of the resulting system is still influenced by uncertainties, which are usually composed of unpredictable parameter variations, external load disturbances, unmodeled and nonlinear dynamics (Barambones et al. 2007).

The classical proportional integral (PI) controllers are the main control technique being used in AC machine drives. In some situations, where there are parametric variations and uncertainty, the PI controller is unable to provide the desired performance (Harnefors et al. 2013). This problem can be solved using adaptive control techniques, artificial neural network (ANN), fuzzy systems and sliding mode controllers (SMC), among others (Vas 1999; Wai and Su 2006; Ravi Teja et al. 2012).

Although the aforementioned techniques present a good performance, the SMC has a simpler design, implementation and lower computational effort based on the maximum effort control. The SMC presents fast response to system input changes, robustness regarding parametric variations and also nonlinear characteristics of the plant. In contrast, the SMC presents an undesired effect called chattering, typically when the signal function is used as switching function. The chattering problem consists in high-frequency oscillations due

to the switching nature of the controller. These oscillations might excite unstable system dynamics (Utkin 1993; Hung et al. 1993).

One of the first papers presenting the SMC basic theory, spreading the concepts and their practical use was published in 1977 (Utkin 1977). Since then, numerous works have been done in order to improve the results in real control systems, specially regarding the chattering reduction issues. In the last years, some techniques are used along with SMC, including adaptive control and intelligent systems like fuzzy and ANN. Sometimes, the use of these techniques increase the controller complexity and computational effort, losing one of the main advantages of SMCs (El-Sousy 2013; Pupadubsin et al. 2012; Saghafinia et al. 2015).

Some authors propose the use of higher-order sliding mode algorithm for chattering reduction. However, it requires higher-order real-time derivatives of the outputs (Levant 1998; Di Gennaro et al. 2014). Other works apply low-pass filter in the SMC output in order to reduce the chattering effect. Nevertheless, it may be hard to define the ideal cutoff frequency, leading to a poor system performance (Park and Kim 1991; Ben Azza et al. 2014).

A simple way to reduce the chattering problem is achieved using other switching function, as saturation. This eliminates the high-frequency chattering with the consequence of losing a certain degree of robustness regarding load disturbances and uncertainties which can be mitigated with appropriate gains in the function. However, steady-state error will always exist (Hung et al. 1993; Mahmoudi et al. 2007).

Another approach on SMC controller is changing the sliding surface. The traditional sliding surface requires an error and its derivative signal. However, in IM speed control, the evaluation of the acceleration signal by means of the sensed speed is very sensitive to noise effects. Stator current measurements are also noisy signals due to the nature of current sensors (Barambones et al. 2007). Unlike the variable structure designs, an integral sliding surface could be used to eliminate the steady-state error defining, then, the integral sliding mode controller (ISMC). Nevertheless, by adding an integral term in the surface, the system might be subject to a phenomenon known as windup. This phenomenon causes high overshoot and undesired oscillations in the system response (Barambones et al. 2007).

In industry, almost all processes are subject to some sort of restriction in control. One of the most common restrictions is the overshoot. Sometimes, high overshoot leads to poor performance. To avoid this problem, an anti-windup method should be used. A good anti-windup design is essential to high-performance IM drive applications, specially involving repeated and quick transitions between different operating regions (Sepulchre et al. 2013).

In order to overcome the drawbacks previously mentioned, a SMC controller is proposed with a sigmoid function as switching function and an integral sliding surface with a new anti-windup method. The proposed anti-windup method takes into account a gain based on a Gaussian function, setting only the range of the integral action. This integral sliding mode controller with a new anti-windup (ISMC-AW) is a structure that presents a low complexity control law, which allows practical implementations to be developed.

2 Model and Control of Induction Motor

2.1 Model of Induction Motor in an Arbitrary Reference Frame

The used mathematical model of IM is written in an arbitrary reference (ω_λ) (Vas 1990):

$$\underline{v}_\mathrm{s} = R_\mathrm{s}\underline{i}_\mathrm{s} + \frac{\mathrm{d}}{\mathrm{d}t}\underline{\psi}_\mathrm{s} + j\omega_\lambda\underline{\psi}_\mathrm{s} \tag{1}$$

$$0 = R_\mathrm{r}\underline{i}_\mathrm{r} + \frac{\mathrm{d}}{\mathrm{d}t}\underline{\psi}_\mathrm{r} + j\left(\omega_\lambda - \omega_\mathrm{r}\right)\underline{\psi}_\mathrm{r} \tag{2}$$

where $\underline{v}_\mathrm{s}$ is the stator voltage vector; $\underline{i}_\mathrm{s}$ and $\underline{i}_\mathrm{r}$ are stator and rotor current vectors, respectively; $\underline{\psi}_\mathrm{s}$ and $\underline{\psi}_\mathrm{r}$ are stator and rotor flux vectors, respectively; R_s and R_r are stator and rotor resistances, respectively; ω_r is the electrical rotor speed; ω_λ is arbitrary synchronous speed and j is the imaginary operator.

The mechanical modeling part of the system is given by Vas (1990):

$$J\frac{\mathrm{d}}{\mathrm{d}t}(\omega_\mathrm{m}) = T_\mathrm{el} - F\omega_\mathrm{m} - T_\mathrm{l} \tag{3}$$

where ω_m is rotor mechanical speed; T_el is the electromagnetic torque; F is the total (rotor axis and load) viscous coefficient; J is the total (rotor and load) momentum of inertia; and T_l is the load torque, applied in machine rotor.

2.2 Indirect Field-Oriented Control

Usually in the field-oriented control of IM, stator flux or rotor flux can be used as reference frame. In this work, the rotor flux is adopted. In the adopted reference frame, the torque and flux control can be directly decoupled. Once the flux is oriented in the rotor flux ψ_r, it has only its direct axis component $\psi_{\mathrm{d}r}$:

$$\underline{\psi}_\mathrm{r} = \psi_{\mathrm{d}r} + j0. \tag{4}$$

Similarly, the electromagnetic torque is Vas (1990):

$$T_\mathrm{el} = K_\omega\psi_{\mathrm{d}r}i_\mathrm{qs} \tag{5}$$

where $K_\omega = (3/2)(L_m/L_s)p$; p is the number of pole pairs; L_m, L_s and L_r are mutual, stator and rotor inductances, respectively.

The synchronous rotor flux component ψ_{dr} is given by:

$$\frac{d}{dt}\psi_{dr} = -\frac{1}{T_r}\left[\psi_{dr} - L_m i_{ds}\right] \tag{6}$$

where $T_r = L_r/R_r$ is the rotor time constant.

In this work, the rotor flux will be kept constant. By means of (6), the rotor flux ψ_{dr} can be controlled indirectly by direct stator current component i_{ds}. Thus, the reference of the control loop is given by:

$$i_{ds}{}^* = \frac{\psi_{dr}{}^*}{L_m} \tag{7}$$

where L_m is the mutual inductance and superscript * denotes the reference value.

The rotor flux instantaneous position is obtained from the relation between electrical rotor speed (ω_r) and rotor slip frequency (ω_{slp}), so the rotor flux synchronous speed (ω_e) can be written as:

$$\omega_r = p\omega_m \tag{8}$$

$$\omega_{slp} = \frac{1}{T_r}\frac{L_m i_{qs}}{\psi_{dr}} \tag{9}$$

$$\omega_e = \omega_r + \omega_{slp}. \tag{10}$$

Flux rotor position (θ_e), necessary to dq axes transformations, is obtained from the integration of (10):

$$\theta_e = \int \omega_e dt. \tag{11}$$

The complete diagram for IFOC control strategy is shown in Fig. 1, where $v_{\alpha s}{}^*$ and $v_{\beta s}{}^*$ are stationary direct and quadrature reference stator voltages, respectively; v_a, v_b and v_c are the three-phase stator voltage.

3 General Concept of Sliding Mode

The main idea of sliding mode control consists in moving the state trajectory of the system toward a predetermined surface called sliding surface, and once it is reached, the system is immune to parametric variations and disturbances, limited to a sort of ranges. This way, the project of the SMC can be divided into two parts: the definition of the adequate sliding surface $S(x)$ and the development of a control law U_c (Shtessel et al. 2014).

In order to satisfy the conditions of convergence to solve the system, or the convergence to the sliding regime, an integral surface $S(x)$ is defined by Slotine and Li (1991):

$$S(x) = \left(\lambda + \frac{d}{dt}\right)^{r-1} \int e\, dt \tag{12}$$

where $e = (x^* - x)$ is the error; x is the system state space; x^* is system state space reference; r is the degree of the sliding mode; and λ is the weighting factor.

A way to analyze the system with the sliding mode control is using the equivalent control method in a generic system described by Mahmoudi et al. (2007):

$$\begin{aligned} \dot{x} &= f(x) + g(x)U_c \\ y &= h(x) \end{aligned} \tag{13}$$

where $x \in \mathbb{R}^n$ is the state space vector; $U_c(t) \in \mathbb{R}^m$ is the input control action; and $y(t) \in \mathbb{R}^p$ is the system output. Thus, by means of analogy it is possible to make a simple analysis in the vector control of the IM (Mahmoudi et al. 2007).

The equivalent control method consists of the division of the control signal U_c in two parts:

$$Uc = U_{equ} + U_n \tag{14}$$

where U_{equ} is the equivalent control action, liable for guaranteeing the convergence of the system and U_n is called switching control action, responsible for assuring the attractiveness of the surface to system state space.

Rewriting (13) by means of (14):

$$\dot{x} = f(x) + g(x)U_{equ} + g(x)U_n. \tag{15}$$

A widely accepted method to prove the convergence of this set of equation is the Lyapunov energy function V. In this case, V is defined as Slotine and Li (1991):

$$V = \frac{1}{2}S^2. \tag{16}$$

For the asymptotic stability of the chosen surface (12) in the equilibrium point ($S = 0$), some conditions must be satisfied:

$$\lim_{S\to\infty} V = \infty \tag{17}$$

$$\dot{V} = S\dot{S} < 0 \quad \text{for} \quad S \neq 0. \tag{18}$$

Condition (17) is clearly satisfied, but for condition (18) it is necessary to consider the existence of $\dot{S}(x)$ for the system described by (15). This case, $\dot{S}(x)$, is Mahmoudi et al. (2007):

$$\begin{aligned} \dot{S}(x) = \frac{\partial S}{\partial x}\frac{dx}{dt} &= \frac{\partial S}{\partial x}[f(x) + g(x)U_{equ}] \\ &+ \frac{\partial S}{\partial x}[g(x)U_n]. \end{aligned} \tag{19}$$

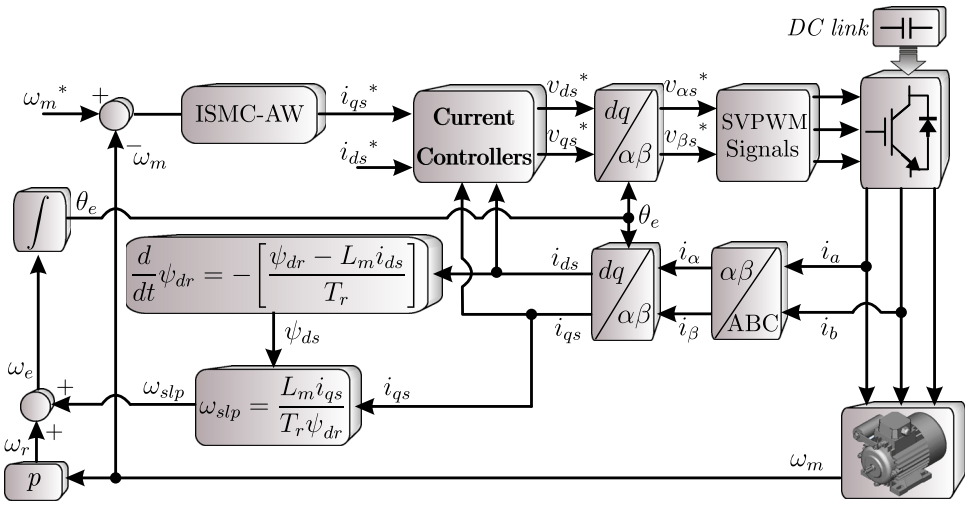

Fig. 1 Overall block diagram of the control scheme for IM

Solving U_{equ} to make the first term of (19) be zero or, i.e., from the definition of equivalent control as the portion of control that is responsible for the set point of the system:

$$U_{\text{equ}} = -\left[\frac{\partial S}{\partial x} g(x)\right]^{-1} \left[\frac{\partial S}{\partial x} f(x)\right]. \tag{20}$$

Typically, U_{equ} is determined off-line with a model that represents the plant as accurately as possible (Barambones et al. 2007). However, the term U_n can be large enough to compensate the uncertainties and assure that the state is attracted to the sliding surface by satisfying the condition (18). In this case, the equivalent control can be understood as a value between the limits $[U_{n\,\min}\ U_{n\,\max}]$ of the switching control (Mahmoudi et al. 2007; Slotine and Li 1991). So, it is possible to restrict the analysis applying (20) in (19) (Mahmoudi et al. 2007):

$$\dot{S}(x) = \frac{\partial S}{\partial x} g(x) U_n. \tag{21}$$

Applying (21) in (18):

$$S(x)\dot{S}(x) = S(x)\frac{\partial S}{\partial x} g(x) U_n < 0. \tag{22}$$

Some switching functions are usually applied to the SMC, like the traditional signal function (23), in order to converge the system to the desired operating point ($S(x) = 0$).

$$U_n = \zeta_{\,\text{M}} \text{sgn}(S(x)). \tag{23}$$

Applying (23) in (22):

$$S(x)\dot{S}(x) = \frac{\partial S}{\partial x} g(x) \zeta_{\,\text{M}} |S(x)| < 0. \tag{24}$$

This way, it is necessary to analyze the term $\frac{\partial S}{\partial x} g(x)$ of the system considered in this work. Once the gain $\zeta_{\,\text{M}}$ is the amplitude of the sign function with positive value, the inequality (24) must be satisfied (Mahmoudi et al. 2007).

4 Proposed ISMC-AW

The proposed ISMC-AW controller is employed in the speed control loop, as shown in Fig. 1.

4.1 Continuous Approximation of Switching Control Law

It is well known that, when the sign function is applied to the SMC, the chattering phenomenon is noticeable. The main reason lies on the discontinuous nature of the sign function and the sampling frequency that is limited by the processor capability (Utkin 1993). Furthermore, the sign function may vary the inverter frequency throughout the operation. One of the most significant consequences of chattering in IM is the degradation of stator currents and, therefore, the electromagnetic torque. The chattering problem affects the overall performance of the system (Hung et al. 1993).

A possible and simple alternative to reduce chattering is the use of an analog sign function, e.g., the saturation function (Hung et al. 1993). This function has a linear region between saturation limits, and the maximum value is abruptly reached. Unlike the traditional saturation function, in this work is proposed the use of the hyperbolic tangent function tan$h$, (Fig. 2). The tan$h$ function has a smoother behavior near the saturation value, making it a good candidate for chattering reduction in noisy control systems, as in the IM control. Choosing appropriate positive values for $\zeta_{\,\text{M}}$ and ϕ in (25), it is possible to modify the amplitude and inclination of the tan$h$ function, respectively. For any application, the gain $\zeta_{\,\text{M}}$ is always the maximum output value of the controller or the saturation value. At the speed control loop developed for the machine, in this work, the value $\zeta_{\,\text{M}} = 2,7$.

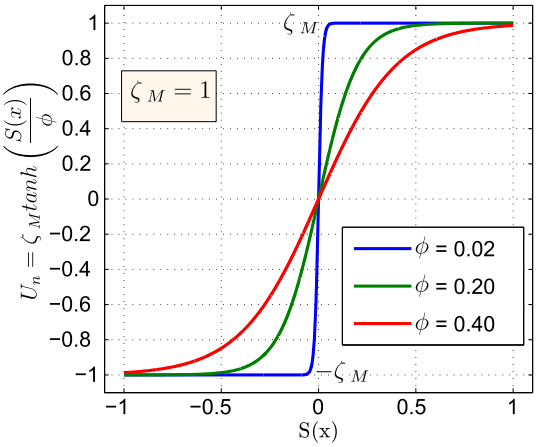

Fig. 2 Hyperbolic tangent function graph

$$U_n = \zeta_{\mathrm{M}} \tanh\left(\frac{S(x)}{\phi}\right). \tag{25}$$

With the help of Fig. 2, it is possible to pick up ϕ in order to tune the controller, so for the speed controller:

$$\phi_{\omega \mathrm{m}} = \phi\, \omega_{\mathrm{M}} \tag{26}$$

where ω_{M} is the maximum shaft speed.

For small speed steady-state error, in this work is used $\phi = 0.025$. Considering $\omega_{\mathrm{M}} = 377$ rad/s for the used machine, $\phi_{\omega \mathrm{m}} \approx 9$.

4.2 Design of the Sliding Surface

The use of hyperbolic tangent as a switching function with the traditional sliding surface (27) introduces steady-state error in the plant output. In this case, the controller is defined as the conventional SMC.

$$S_{\omega_{\mathrm{m}}} = e_{\omega m}. \tag{27}$$

To solve this problem, the steady-state error can be eliminated by means of an integral compensator in the sliding surface. Considering the general integral surface (12) for mechanical speed control loop:

$$S_{\omega_{\mathrm{m}}} = \ e_{\omega m} + \lambda_{\omega \mathrm{m}} \int e_{\omega \mathrm{m}}\ \mathrm{d}t. \tag{28}$$

By means of sliding mode theory, the robustness property of conventional SMC related to parametric variations and external disturbances can only be achieved after the occurrence of sliding mode. Nevertheless, during the reaching phase, there is no guarantee of robustness. Integral sliding mode seeks to eliminate the reaching phase by enforcing sliding mode throughout the entire system response (Utkin et al. 2009).

4.3 New Anti-windup Method

Generally, controllers that have an integral term in their structure are subject to a problem known as windup. When it is in closed-loop control, the integrative portion may have an improper accumulation of error, which is not due to the difference between the signal reference and current value. In conventional PI controllers, when the control signal is saturated, the integrative term may continue to integrate the error regardless of system output. The problem occurs mainly when there is a great variation in the reference signal. Sometimes, this phenomenon can provide inadequate performance of the system, generating responses with high overshoot and settling time (Astrom and Hagglund 2005; Costa et al. 2015).

According to the definition of sliding mode systems, the integrative portion should be inserted only on the sliding surface (Utkin et al. 2009). Thus, the anti-windup could be accomplished by means of saturation on the accumulated error. However, for small reference signals, it shall take a long time until the accumulated error reaches the saturation limit. This way, the overshoot would still be high, as well as the settling time.

For the PI controller, some methods to fix this problem are well known, such as back-calculation, integrator clamping, feed-forward method and full state prediction (Li et al. 2011; Scottedward Hodel and Hall 2001). Although there are a large number of methods for the PI controller, the same may not be said to the ISMC.

Once the controller output is already saturated by the switching function (hyperbolic tangent), a simple way to solve this problem could be by means of conditional integration or integrator clamping (Li et al. 2011). In this case, the integral action is switched on or off depending on the linear range or the saturation range. However, with this method on the sliding surface, it is difficult to choose an integral gain $\lambda_{\omega \mathrm{m}}$ to achieve a good anti-windup performance for all range of operation.

Being able to act only on the surface in sliding mode systems turns the problem more complex. Because of this, the proposed method is similar to the integrator clamping method. However, instead of saturation, here is considered a gain $\beta_{\omega \mathrm{m}}$, which sets the area of activity of the integrative portion, such that the accumulation of error is smaller, and therefore, it does not affect the system. Furthermore, the integral gain $\lambda_{\omega \mathrm{m}}$ may vary only within the designed limits.

In this context, the gain $\beta_{\omega \mathrm{m}}$, which is a positive function, is inserted on the sliding surface (29).Thus, it is possible to adjust $\beta_{\omega \mathrm{m}}$ based on the gain σ, as shown in Fig. 3. With help of Fig. 3 and considering $\omega_{\mathrm{M}} = 377$ rad/s, in this work is adopted $\sigma = 300$.

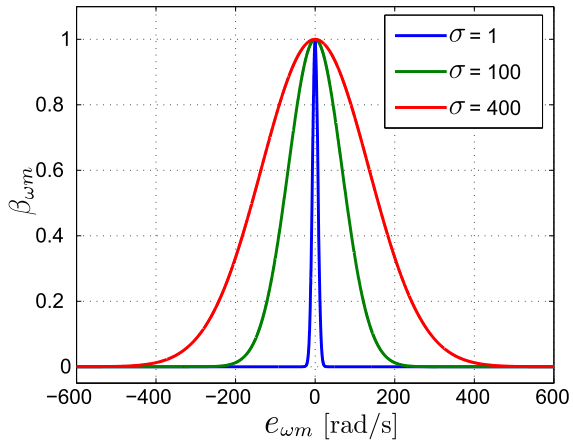

Fig. 3 The gain $\beta_{\omega m}$ based on Gaussian function with different values of σ

$$S_{\omega_m} = e_{\omega m} + \lambda_{\omega m} \int \beta_{\omega m} e_{\omega m} \, dt \tag{29}$$

$$\beta_{\omega m} = e^{\frac{-e_{\omega m}{}^2}{\sigma}} \tag{30}$$

4.4 Mathematical Analysis

Since the proposed controller demands $\zeta_M > 0$, the attractiveness of the sliding surface is limited to the condition (22), and thus, only the surface (29) shall be analyzed. As the time constant of mechanical system is by far greater than the electrical system's time constant, it is possible to make separated analysis for the speed control loop (Panchade et al. 2011).

Thus, (3) must be written as (13) in order to verify that it satisfies (24). Solving (24) and considering (29), it yields:

$$\frac{\partial S_{\omega_m}}{\partial \omega_m} \frac{K_w \psi_{ds}}{J} = -(1 + \lambda_{\omega m} t) \frac{K_w \psi_{ds}}{J} < 0 \tag{31}$$

where: t is time.

The gains $\lambda_{\omega m}$ and $\beta_{\omega m}$ will always be positive as well as the controlled rotor flux (ψ_{ds}). As can be seen in Fig. 3, when the system reaches the sliding surface the gain $\beta_{\omega m}$ tends to one. However, in the reaching phase, $\beta_{\omega m}$ tends to be zero, behaving as a conventional SMC.

5 Results and Discussion

In this section, the performance of the proposed ISMC-AW based on IM drives has been investigated by means of simulation and experiments. To show the superior performance achieved by the proposed ISMC-AW, it shall be compared with the conventional SMC controllers and also a finely tuned PI.

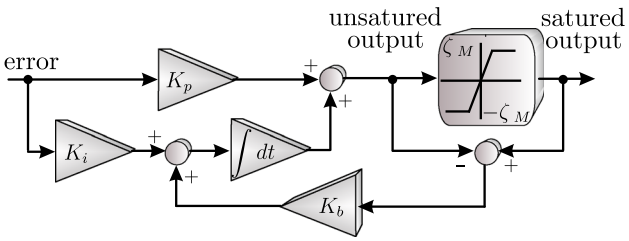

Fig. 4 Structure of anti-windup PI controller

The PI controller with back-calculation anti-windup method is applied (Fig. 4) (Astrom and Hagglund 2005; Costa et al. 2015). Initially, the PI controller is tuned by Ziegler–Nichols method based on stability boundary like in Saghafinia et al. (2015). Afterward, the gains K_p, K_i, K_b and ζ_{sat} are fine-tuned using the method suggested by Astrom and Hagglund (2005).

The rotor flux of the IM has been set to its nominal value of 0.7 $[Wb]$, keeping the flux current command $i_{ds}{}^*$ to a constant value of 1$[A]$. On the other hand, the electromagnetic torque current command, $i_{qs}{}^*$, has been limited to 2, 7$[A]$, in order to provide protection against overcurrents in the IM.

5.1 Simulation Results

The simulation results were obtained utilizing MATLAB/Simulink ^{TM} software, using the parameters shown in "Appendix 1," for the controllers, and "Appendix 2," for the IM. The sampling frequency is 20kHz for current data acquisition and 5kHz for the control loop and PWM switching frequency.

For simulation tests, several cases including parametric variations and external load disturbance are considered. If not mentioned, all other parameters are considered to be nominal in all the cases.

5.1.1 Parameter Variations

Robustness to parametric variations is a common term for various aspects of control in IM, e.g., the rotor time constant has a great influence on both the steady-state performance and the dynamic regulation. Because of the thermal effect, the rotor resistance can reach twice its nominal value; hence, the relative speed error caused by rotor time constant error is non-negligible (Wang et al. 2014). So, rotor resistance R_r is increased twice its nominal value from the beginning. The mechanical speed responses to 2200, −1200 and −50 RPM for the proposed ISMC-AW and the tuned PI controller are shown in Fig. 5.

The proposed ISMC-AW has faster response than the tuned PI controller for all the speed steps and does not present high overshoot under parametric variation. Besides, the anti-

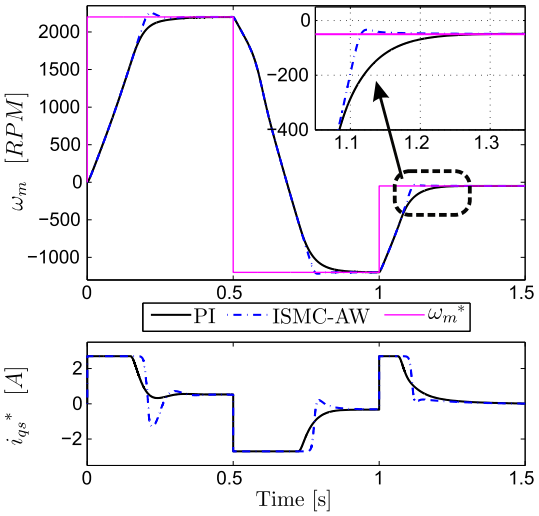

Fig. 5 Simulation result at mechanical speed responses at 2200, −1200 and −50 of ω_m, ω_m^* and i_{qs}^*

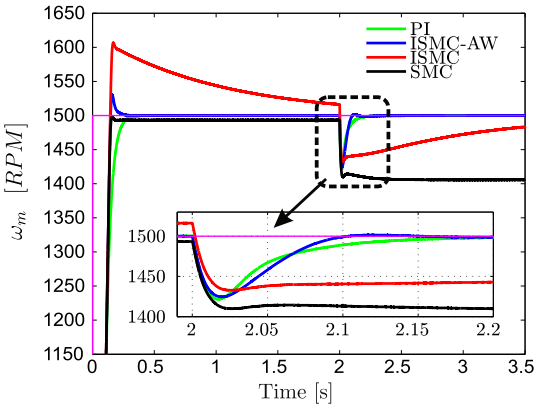

Fig. 6 Simulation result at 1500 RPM for tuned PI, conventional SMC, ISMC and the proposed ISMC-AW of ω_m

windup technique works well even in low mechanical speeds. In this case, it is noticeable the maximum control effort without chattering in the reference current signal i_{qs}^* for the proposed ISMC-AW.

5.1.2 Load Variation at Constant Speed

In this situation, four controllers are employed: the proposed ISMC-AW, ISMC using a sliding surface (28), the conventional SMC without an integral term in the sliding surface (27) and the tuned PI controller (Fig. 4). The performance of the machine is shown in Fig. 6 with a step change in the speed reference from 0 to 1500 RPM. The load torque is changed from 0 to 2 N.m. at $t = 2$s.

As seen in Fig. 6, the use of a hyperbolic tangent function as a switching function minimizes the chattering problem in all SMC controllers.

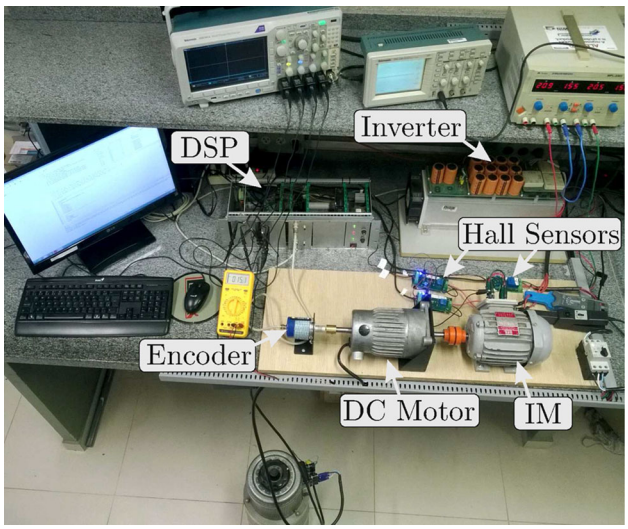

Fig. 7 System configuration for the experimental setup

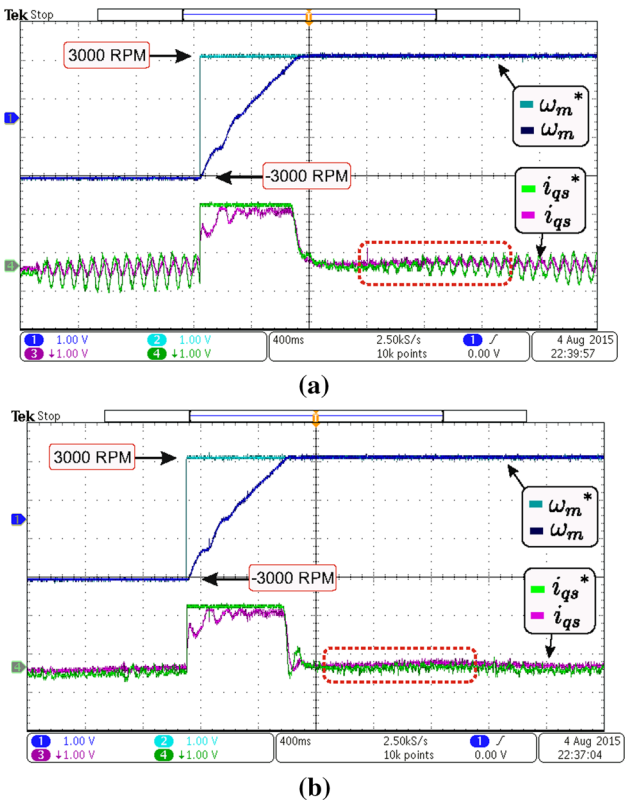

Fig. 8 Experimental result at reversion speed from −3000 to 3000 RPM with the rotor resistance value of three times the nominal value using **a** tuned PI controller **b** the ISMC-AW

Even a small integrator gain $\lambda_{\omega m}$ in ISMC, compared to the gain $\lambda_{\omega m}$ used in ISMC-AW, provides high overshoot. With the proposed ISMC-AW, the overshoot is smaller than 2 %. On the other hand, the conventional SMC shows faster settling time without overshoot but presents larger steady-state speed error when load is applied. In terms of robustness

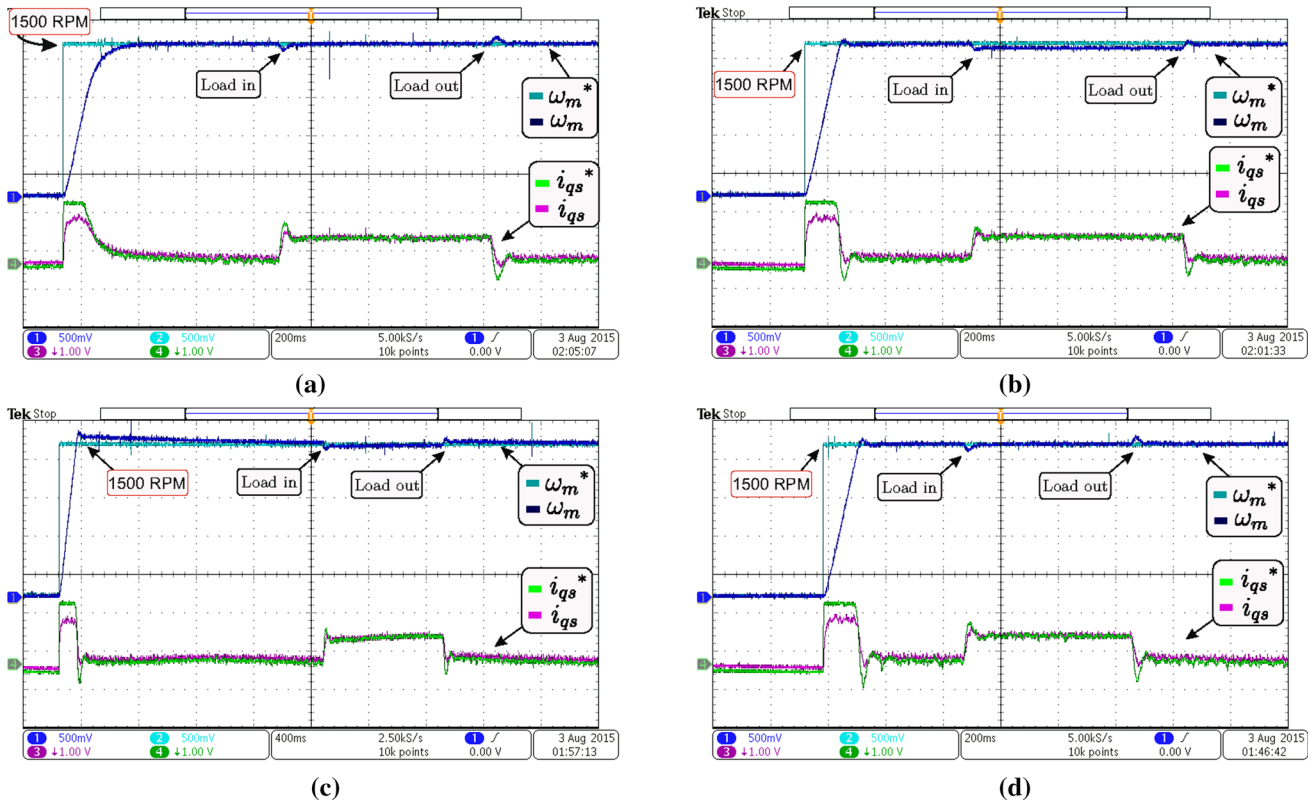

Fig. 9 Experimental result at 1500 RPM with load variation using **a** tuned PI controller, **b** SMC, **c** ISMC and **d** ISMC-AW

to load disturbance, the proposed ISMC-AW exhibits a better performance compared to the other SMC controllers.

Although a tuned PI can provide a good system response, as in Fig. 6, it requests a higher effort in order to tune its parameters, whereas the ISMC-AW requests a lower effort to tune it.

5.2 Experimental Results

The experimental setup is shown in Fig. 7. It is composed by 2.2-kVA 380-V commercial inverter and 1 HP IM (parameters shown in "Appendix 2"). A generator with resistive load is used as mechanical load. Control algorithms are running on a floating-point DSP F28377D from Texas Instruments.

Hall sensors are employed for current feedback. The sampling frequency is 20kHz for current signals acquisition and 5kHz for the control loop and PWM switching frequency. The rotor speed is monitored using an incremental encoder. All experimental results are obtained using the parameters shown in "Appendix 1" for the controllers.

5.2.1 Reversion Speed with Parametric Variation

In order to evaluate the robustness of the proposed controller, the rotor resistance R_r value is changed to three times the nominal value, at the beginning of the DSP algorithm. To show the dynamic performance, a reversal speed step from 3000 to −3000 RPM is presented (Fig. 8).

In such case, the reference and actual values of speed and the i_{qs} currents axes are shown in Fig. 8a, b for the tuned PI controller and the proposed ISMC-AW, respectively. It can be seen that the proposed ISMC-AW has good speed response since speed errors are still small even at operation under parametric variations. From this experimental result, there are no chattering phenomena in the control efforts and favorable tracking response can be obtained under the occurrence of uncertainties. Apparently, ISMC-AW and the tuned PI present similar ω_m response; however, analyzing i_{qs} current, one can be noticed that oscillations are presented only by the tuned PI controller. Thus, the harmonic losses of the IM with the proposed ISMC-AW will be lower if compared to the tuned PI.

5.2.2 Load Variation at Constant Speed

The second experiment presents the start-up performance with a speed step from 0 to 1500 RPM. The load torque is varied from 0 to 1 N.m.

In order to illustrate the industrial environment where commercial inverters generally apply PI controllers, the

response of a tuned PI is presented in Fig. 9a. Thanks to the applied anti-windup technique (Fig. 4), the system presents a damped response to a step in mechanical speed.

Although the tuned PI presents a good dynamic performance in step speed change, the proposed ISMC-AW (Fig. 9d) achieves lower settling time with minimal overshoot.

Figure 9b shows the results for the conventional SMC, which also has faster response of ω_{m} and better settling time than the tuned PI controller. However, since the conventional SMC does not have an integral gain $\lambda_{\omega \mathrm{m}}$, when the load is applied, the steady-state error becomes more noticeable. Furthermore, the SMC is more susceptible to load disturbances than the proposed ISMC-AW.

The steady-state error introduced by the lack of integral gain on the SMC can be reduced by tuning the slope gain ϕ of the tan$h$ switching function, but this maneuver increases the chattering issue.

The results for ISMC are shown in Fig. 9c. It has the highest overshoot and the slowest dynamics of all presented controllers in Fig. 9. In this type of controller, small gains in the integral term $\lambda_{\omega \mathrm{m}}$ lead to slow dynamics to eliminate the steady-state error with low overshoot, and with large integrative gain, the opposite is valid. Thus, tuning the gains becomes a difficult process and does not provide high dynamic performance, showing the difficulty of working in the sliding surface with the integral term.

The consequence of the maximum control effort, characteristic of sliding mode systems, can be seen in Fig. 9d, in the fast response of i_{qs}^{*} without chattering and presenting few oscillations, responding quickly to load disturbance. The proposed ISMC-AW has fast settling time with low overshoot, without steady-state error, thus eliminating the disadvantages of SMC and ISMC. Therefore, in general, the ISMC-AW becomes the best option.

6 Conclusions

This work presents an ISMC-AW in the speed control loop of the IM with wide operational range, robust to parametric variations, by means of IFOC technique.

As presented in this work, a well-tuned PI can provide a good system response. However, in the speed control loop, it demands a higher effort in order to tune its parameters more than the ISMC-AW. The PI controller requires IM parameters or experimental tests to perform the tuning, whereas the ISMC-AW only needs nominal data of the machine, such as speed and maximum allowed current.

Despite a sliding surface being normally composed by acceleration with the error or only the error in the vector control of IM, this work presents a non-usual integral sliding surface. The applied integral sliding surface with an anti-windup method presented good chattering reduction for this application, with minimal system performance degradation. In addition, good operational characteristics for the IM in different situations are presented, regarding the use of different switching functions in other works (Mahmoudi et al. 2007; Barambones et al. 2007; Saghafinia et al. 2015).

According to the obtained results, the proposed ISMC-AW offers a stable speed response without chattering, even in situations that present parametric variations. In addition, the proposed ISMC-AW combines the advantages of conventional SMC controllers, as the maximum control effort without the basic disadvantages of steady-state error and high overshoot and without requiring IM parameters as happens in other works (Saghafinia et al. 2015; Barambones et al. 2007).

Acknowledgments The authors acknowledge the support granted by CAPES.

Appendix 1: Parameters of the Controllers

ISMC-AW (ω_{m})			
$\zeta_{\mathrm{M}} = 2.7$	$\phi = 9$	$\lambda_{\omega \mathrm{m}} = 25$	$\sigma = 300$
ISMC (ω_{m})			
$\zeta_{\mathrm{M}} = 2.7$	$\phi = 9$		$\lambda_{\omega \mathrm{m}} = 1$
CONVENTIONAL SMC (ω_{m})			
$\zeta_{\mathrm{M}} = 2.7$		$\phi = 9$	
TUNED PI (ω_{m})			
$\zeta_{\mathrm{sat}} = 2.7$	$K_p = 0.22$	$K_i = 4.2452$	$K_b = 0.25$
PI current controllers (i_{ds},i_{qs})			
$\zeta_{\mathrm{sat}} = 311$	$K_p = 12.79$		$K_i = 2256$

Appendix 2: Induction Motor Data

Parameter	Value	Unit
Power	1	HP
R_{s}	7.5022	Ω
R_{r}	4.8319	Ω
(L_{s} e L_{r})	718.5	mH
L_{m}	694.1	mH
p	1	
J	$2.028\ 10^{-3}$	Kg m^2
F	$1.362\ 10^{-3}$	N m s
Voltage	220	V

References

Astrom, K. J., & Hagglund, T. (2005). *Advanced PID control*. Research Triangle Park, NC: Instrument Society of America.

Barambones, O., Garrido, A. J., & Maseda, F. J. (2007). Integral sliding-mode controller for induction motor based on field-oriented control theory. *IET Control Theory and Applications*, *1*(3), 786–794.

Ben Azza, H., Zaidi, N., Jemli, M., & Boussak, M. (2014). Development and experimental evaluation of a sensorless speed control of SPIM using adaptive sliding mode-MRAS strategy. *IEEE Journal of Emerging and Selected Topics in Power Electronics*, *2*(2), 319–328.

Costa, B. L. G., Angélico, B. A., Goedtel, A., Castoldi, M. F., & Graciola, C. L. (2015). Differential evolution applied to DTC drive for three-phase induction motors using an adaptive state observer. *Journal of Control, Automation and Electrical Systems*, *26*(4), 403–420.

Di Gennaro, S., Rivera Dominguez, J., & Meza, M. A. (2014). Sensorless high order sliding mode control of induction motors with core loss. *IEEE Transactions on Industrial Electronics*, *61*(6), 2678–2689.

El-Sousy, F. F. M. (2013). Adaptive dynamic sliding-mode control system using recurrent RBFN for high-performance induction motor servo drive. *IEEE Transactions on Industrial Informatics*, *9*(4), 1922–1936.

Harnefors, L., Saarakkala, S. E., & Hinkkanen, M. (2013). Speed control of electrical drives using classical control methods. *IEEE Transactions on Industry Applications*, *49*(2), 889–898.

Hung, J. Y., Gao, W., & Hung, J. C. (1993). Variable structure control: A survey. *IEEE Transactions on Industrial Electronics*, *40*(1), 2–22.

Levant, A. (1998). Robust exact differentiation via sliding mode technique. *Automatica*, *34*(3), 379–384.

Li, X. L., Park, J. G., & Shin, H. B. (2011). Comparison and evaluation of anti-windup PI controllers. *Journal of Power Electronics*, *11*(1), 45–50.

Mahmoudi, M. O., Madani, N., Benkhoris, M. F., & Boudjema, F. (2007). Cascade sliding mode control of a field oriented induction machine drive. *The European Physical Journal Applied Physics*, *7*(3), 217–225.

Panchade, V. M., Waghmare, L., Patre, B. M., & Bhogle, P. P. (2011). *Robust control, theory and applications* (vol. 1). InTech

Park, Min-Ho, & Kim, Kyung-Seo. (1991). Chattering reduction in the position control of induction motor using the sliding mode. *IEEE Transactions on Power Electronics*, *6*(3), 317–325.

Pupadubsin, R., Chayopitak, N., Taylor, D. G., Nulek, N., Kachapornkul, S., Jitkreeyarn, P., et al. (2012). Adaptive integral sliding-mode position control of a coupled-phase linear variable reluctance motor for high-precision applications. *IEEE Transactions on Industry Applications*, *48*(4), 1353–1363.

Ravi Teja, A. V., Chakraborty, C., Maiti, S., & Hori, Y. (2012). A new model reference adaptive controller for four quadrant vector controlled induction motor drives. *IEEE Transactions on Industrial Electronics*, *59*(10), 3757–3767.

Saghafinia, A., Ping, H. W., Uddin, M. N., & Gaeid, K. S. (2015). Adaptive fuzzy sliding-mode control into chattering-free IM drive. *IEEE Transactions on Industry Applications*, *51*(1), 692–701.

Scottedward Hodel, A., & Hall, C. (2001). Variable-structure PID control to prevent integrator windup. *IEEE Transactions on Industrial Electronics*, *48*(2), 442–451.

Sepulchre, R., Devos, T., Jadot, F., & Malrait, F. (2013). Antiwindup design for induction motor control in the field weakening domain. *IEEE Transactions on Control Systems Technology*, *21*(1), 52–66.

Shtessel, Y., Edwards, C., Fridman, L., & Levant, A. (2014). *Sliding mode control and observation*. Hardcover.

Slotine, J. J. E., & Li, W. (1991). *Applied nonlinear control*. New Jersey: Prentice Hall.

Utkin, V. (1977). Variable structure systems with sliding modes. *IEEE Transactions on Automatic Control*, *22*(2), 212–222.

Utkin, V. (1993). Sliding mode control design principles and applications to electric drives. *IEEE Transactions on Industrial Electronics*, *40*(1), 23–36.

Utkin, V. I., Guldner, J., & Shi, J. (2009). *Sliding mode control in electromechanical systems* (2nd ed.). Boca Raton: CRC Press.

Vas, P. (1990). *Vector control of AC machines. Monographs in electrical and electronic engineering*. Oxford: Clarendon Press.

Vas, P. (1999). *Artificial-intelligence-based electrical machines and drives: Application of fuzzy, neural, fuzzy-neural, and genetic-algorithm-based techniques*. Oxford: Oxford University Press.

Wai, R. J., & Su, K. H. (2006). Adaptive enhanced fuzzy sliding-mode control for electrical servo drive. *IEEE Transactions on Industrial Electronics*, *53*(2), 569–580.

Wang, K., Chen, B., Shen, G., Yao, W., Lee, K., & Lu, Z. (2014). Online updating of rotor time constant based on combined voltage and current mode flux observer for speed-sensorless AC drives. *IEEE Transactions on Industrial Electronics*, *61*(9), 4583–4593.